BIOCHEMISTRY
including biophysical chemistry & molecular biology

Article

pubs.acs.org/biochemistry

Differential Binding between PatS C-Terminal Peptide Fragments and HetR from *Anabaena* sp. PCC 7120

Erik A. Feldmann,[†] Shuisong Ni,[†] Indra D. Sahu,[†] Clay H. Mishler,[†] Jeffrey D. Levengood,[†] Yegor Kushnir,[†] Robert M. McCarrick,[†] Gary A. Lorigan,[†] Blanton S. Tolbert,[†] Sean M. Callahan,[‡] and Michael A. Kennedy*[,†]

[†]Department of Chemistry and Biochemistry, Miami University, Oxford, Ohio 45056, United States

[‡]Department of Microbiology, University of Hawaii, Honolulu, Hawaii 96822, United States

ABSTRACT: Heterocyst differentiation in the filamentous cyanobacterium *Anabaena* sp. strain PCC 7120 occurs at regular intervals under nitrogen starvation and is regulated by a host of signaling molecules responsive to availability of fixed nitrogen. The heterocyst differentiation inhibitor PatS contains the active pentapeptide RGSGR (PatS-5) at its C-terminus considered the minimum PatS fragment required for normal heterocyst pattern formation. PatS-5 is known to bind HetR, the master regulator of heterocyst differentiation, with a moderate affinity and a submicromolar dissociation constant. Here we characterized the affinity of HetR for several PatS C-terminal fragments by measuring the relative ability of each fragment to knockdown HetR binding to DNA in electrophoretic mobility shift assays and using isothermal titration calorimetry (ITC). HetR bound to PatS-6 (ERGSGR) >30 times tighter (K_d = 7 nM) than to PatS-5 (K_d = 227 nM) and >1200 times tighter than to PatS-7 (DERGSGR) (K_d = 9280 nM). No binding was detected between HetR and PatS-8 (CDERGSGR). Quantitative binding constants obtained from ITC measurements were consistent with qualitative results from the gel shift knockdown assays. CW EPR spectroscopy confirmed that PatS-6 bound to a MTSL spin-labeled HetR L252C mutant at a 10-fold lower concentration compared to PatS-5. Substituting the PatS-6 N-terminal glutamate to aspartate, lysine, or glycine did not alter binding affinity, indicating that neither the charge nor size of the N-terminal residue's side chain played a role in enhanced HetR binding to PatS-6, but rather increased binding affinity resulted from new interactions with the PatS-6 N-terminal residue peptide backbone.

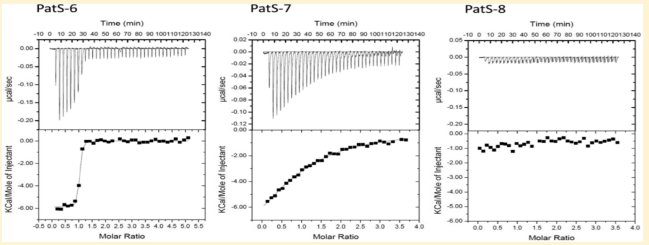

Cyanobacteria are a diverse group of organisms known to exist on Earth for more than 2 billion years[1] and were partially responsible for the oxidation of the planet's atmosphere by photosynthesis.[2] In addition, many species of cyanobacteria fix N_2 gas,[3] an essential step in the nitrogen cycle, contributing to the pool of organic compounds eventually used in synthesis of nucleic and amino acids as well as numerous other biomolecules.[4] Under nitrogen-starved conditions, the filamentous cyanobacterium *Anabaena* sp. strain PCC 7120 differentiates vegetative cells into specialized cells called heterocysts,[5] in order to facilitate nitrogen fixation in heterocysts while maintaining photosynthesis in vegetative cells. Differentiation of vegetative cells into heterocysts is restricted to ∼10% of cells along the filament spaced in a regular pattern.[5] Development of heterocysts and maintenance of the pattern appears to be tightly regulated by a network of signaling molecules responsive to the amount of fixed nitrogen available.[6−8]

Diffusible inhibitors of heterocyst differentiation are thought to play an important role in pattern formation via the establishment of inhibitor gradients that promote destruction of positive regulatory factors for heterocyst differentiation.[9,10] The PatS peptide and HetN protein are two inhibitors that contribute to establishing this regulatory gradient in *Anabaena*.[11] PatS is a 13- or 17-residue (ambiguity due to two potential ATG start codons[12]) peptide required for initial pattern formation[13] and contains the pentapeptide RGSGR at its C-terminus. PatS has been postulated to control the heterocyst pattern by lateral inhibition[8] via the RGSGR motif, which has been shown to be the minimum sequence required for the normal heterocyst patterned phenotype *in vivo*.[12] HetN is a 287-amino acid protein also containing the RGSGR sequence but is not required for initial patterning. Instead, HetN is necessary for proper heterocyst-pattern maintenance during cellular growth and filament elongation afterward.[14] However, proteolytic machinery capable of processing PatS or HetN to smaller peptides has yet to be identified. In addition, the active forms of PatS and HetN unfortunately have also not been successfully isolated and are still unknown.

HetR is a 299-amino acid homodimeric protein that acts as a positive regulator,[15] considered the master regulatory switch for initiation of heterocyst differentiation,[16] and has recently been identified as a direct binding partner for the RGSGR carboxyl terminus of PatS (PatS-5).[17] HetR is an autoregulatory

Received: February 17, 2012
Revised: March 6, 2012
Published: March 7, 2012

   dx.doi.org/10.1021/bi300228n | *Biochemistry* 2012, 51, 2436−2442

transcription factor constitutively expressed at low levels in every cell along the filament[18] and is responsible for activating expression of multiple downstream genes.[15] However, transcription of *hetR* is tightly regulated and is turned over rapidly in *Anabaena*.[19] Transcription of *hetR* is regulated temporally and spatially.[16,18] Under nitrogen starvation, *hetR* transcript levels begin to increase 0.5 h after nitrogen step-down and continue up to a 5-fold increase by 6−18 h.[15,20] Gradients of HetR are established along the filament where a maximum is reached midway between differentiated heterocysts,[11] which also predicted to coincide with a minimum in RGSGR concentration,[11] and it is here that a vegetative cell is initiated to differentiate into a heterocyst. It has been suggested that these gradients of processed RGSGR-containing peptide forms of PatS and HetN promote the post-translational degradation of HetR[20] and consequently play a role in controlling the HetR gradient.[11]

There are four transcriptional start positions (tsps) of *hetR* in *Anabaena* at nucleotides −728, −696, −271, and −184 (relative to the translational start site), and correspondingly each tsp leads to expression of a unique *hetR* mRNA transcript.[20] The −184 tsp transcript is involved in maintenance of basal levels of *hetR* under all growth conditions.[20,21] Transcripts starting from the −728 and −696 tsps are also expressed at low levels under nitrogen replete conditions[20,21] but are significantly upregulated by NrrA under nitrogen starvation.[22,23] NrrA is the response regulatory protein activated by NtcA.[22,23] NtcA is the global nitrogen regulatory protein that responds to 2-oxoglutarate accumulation when *Anabaena* is nitrogen starved[24] and is also required for expression of *hetR* from −728 tsp.[21] The −271 tsp appears to be the only position that requires functional HetR availability[20] and is the only one of the four transcripts that is regulated spatially along the filament.[16] HetR was also found to have *in vitro* binding activity with DNA around the −271 tsp.[25] Accordingly, the PatS and HetN inhibitors have been shown to have a negative effect on *hetR* transcription from tsp −271, and it has been suggested that PatS may regulate patterning by preventing HetR from activating transcription at this tsp, thus contributing further to establishment of the HetR gradient.[16] For these reasons, the −271 tsp is considered the site of HetR autoregulation.

The RGSGR pentapeptide appears to play multiple roles in HetR-related regulation. In addition to promoting HetR destruction, PatS-5 inhibits HetR DNA-binding activity *in vitro*.[17,25,26] This appears to be accomplished from tight binding between the peptide and HetR, which is capable of binding two PatS-5 molecules per HetR homodimer. It also appears that the PatS-5 binding site on HetR is in the proximity of the C-terminal amino acid region R250-D256 based on EPR-based cysteine scanning mutagenesis studies[17] guided by *in vivo* observations that conservative mutations of HetR in this region exhibited differential PatS-5 sensitivity.[26] The recent report of the HetR crystal structure from *Fischerella* MV11 has also modeled this C-terminal area, among other sites, to be likely candidates for the PatS-5 binding site based on Nest predictions from existing protein−peptide binding surfaces.[27] Structures of the HetR−PatS complex or any HetR−DNA complexes, however, remain unknown at this time.

Isothermal titration calorimetry (ITC) has proven to be a valuable technique for studying thermodynamics of protein−protein/peptide/nucleic acid/small molecule interactions particularly exemplified by the drug discovery industry.[28] Such information is valuable when comparing binding interactions of peptide ligands to receptor targets and can be used to provide insight into the binding mechanism.[29,30] When coupled with other biophysical strategies like electron paramagnetic resonance (EPR) spectroscopy, nuclear magnetic resonance spectroscopy, and X-ray crystallography, ITC can be a powerful tool for understanding the fine molecular intricacies of biological processes.

In this report we used ITC and EPR to investigate the *in vitro* HetR binding affinity to several C-terminal PatS fragments of varying length for both the native PatS sequence and for selected amino acid substitutions. We also studied the relative ability of these peptides to disrupt the DNA binding activity of HetR using electrophoretic mobility shift assay (EMSA) knockdown experiments. Surprisingly, our data indicated that HetR binds to PatS-6 with more than 30 times greater affinity compared to PatS-5, which raises important new questions as to what is the active form of PatS *in vivo*. These surprising results, and their implications, are discussed in detail below.

MATERIALS AND METHODS

Cloning, Expression, and Purification of HetR Protein and Preparation of PatS Peptide. Cloning, overexpression, and purification of recombinant soluble HetR were performed as described previously.[17] DNA binding was assessed using electrophoretic mobility shift assays as described previously.[17] The complementary oligonucleotides for the *hetP*-29-mer were synthesized and HPLC purified by Integrated DNA Technologies (Coralville, IA) at 250 nmol scale synthesis for each strand (forward sequence: 5′-GTAGGCGAGGGGTCTAACCCCTCATTACC-3′ and reverse sequence: 5′-GGTAATGAGGGGTTAGACCCCTCGCCTAC-3′). Double-stranded *hetP*-29-mer was annealed by suspending equal stoichiometric concentrations of forward and reverse strands together and heating to 85 °C for 10 min, followed by slow cooling to room temperature. All native and mutant PatS peptides were custom synthesized and purified by Peptide2.0 (Chantilly, VA) on a 5 mg scale and suspended in 100% nanopure H_2O to stock 10 mM concentrations.

EPR Spectroscopy. Generation of purified 252C HetR protein (C48A, L252C double mutant) and subsequent site-directed spin-labeling with the nitroxide spin radical (1-oxyl-2,2,5,5-tetramethyl-pyrrolin-3-yl)methyl methanethiosulfonate (MTSL), (Toronto Research Chemicals Inc.) was performed as described previously.[17] Spin-labeled 252C HetR was concentrated to 200 μM prior to EPR measurements using an Amicon Ultra membrane filter (Millipore). Approximately 30 mL of the HetR and HetR−PatS complexes was drawn into 1.1 mm internal diameter (1.6 mm external diameter) quartz capillaries. Capillaries were placed into 3 mm internal diameter quartz EPR tubes and inserted into the microwave cavity. CW EPR spectra were collected at the Ohio Advanced EPR Laboratory at X-band on a Bruker EMX CW-EPR spectrometer using an ER041xG microwave bridge and ER4119-HS cavity coupled with a BVT 3000 nitrogen gas temperature controller (temperature stability ±0.2 K). CW EPR spectra were collected by signal averaging 15 42-s field scans (consisting of 1024 points and 40 ms time constants and conversion times) with a center field of 3370 G and sweep width of 100 G, microwave frequency of 9.5 GHz, modulation frequency of 100 kHz, modulation amplitude of 1 G, and microwave power of 1 mW at 298 K. EPR spectral simulations to extract best-fit values of the dynamics properties (Table 2) were performed as described previously.[17,31−35]

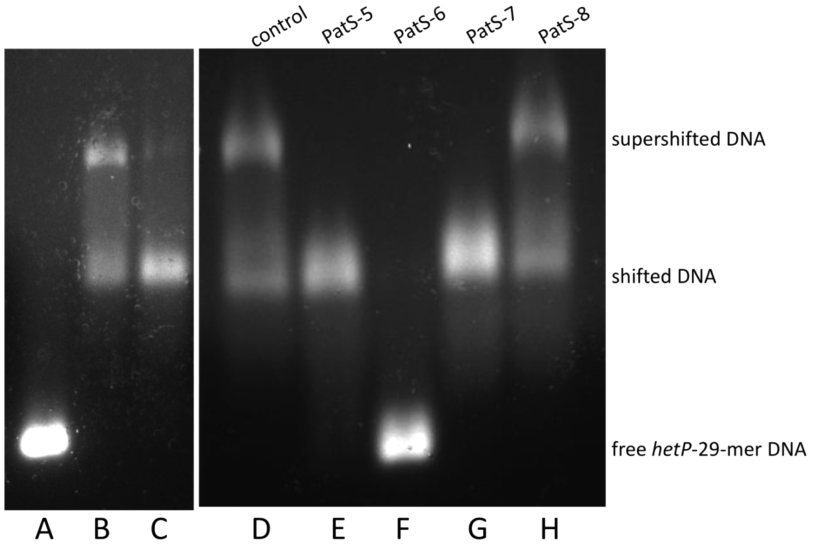

Figure 1. EMSA knockdown gel of PatS C-terminal peptides with the HetR-*hetP*-29-mer DNA complex. Lane A consists of the *hetP*-29-mer DNA alone, lane B contains a 4:1 HetR:*hetP*-29-mer DNA complex, lane C contains a 3:1 HetR:*hetP*-29-mer DNA complex, lane D consists of the 4:1 HetR-*hetP*-29-mer DNA complex control sample, lane E is the complex incubated with a 1:1 ratio (relative to HetR) of PatS-5, lane F is 1:1 incubation with PatS-6, lane G is 1:1 incubation with PatS-7, and lane H is 1:1 incubation with PatS-8. The bottom band represents free *hetP*-29-mer DNA, the middle band represents the primary shifted species of the HetR-*hetP*-29-mer DNA complex, and the top band represents the supershifted species of the complex.

ITC Calorimetry. ITC data were collected at 25 °C on a VP-ITC titration calorimeter (Microcal, Northampton, MA), and the resulting isotherms were deconvoluted and fit using the ORIGIN for ITC software package (Microcal, Piscataway, NJ) provided with the instrument. It was necessary to purify a large homogeneous batch of HetR in order to make a fair comparison between peptides. Several passages of HetR were made through a gel filtration column (Pharmacia Superdex200 HiLoad size exclusion column), and once enough was collected, the HetR stock was dialyzed overnight into buffer containing 1 M NaCl, 10% (w/v) glycerol, 10 mM Tris pH 7.8, and 300 mM imidazole. This reference buffer was later used in the reference cell of the ITC titration as well as for diluting and equilibrating concentrated stocks of synthetic PatS peptides for the ITC titrant. All peptides were diluted to a final concentration of 100 μM with the exception of PatS-6nD, which required 300 μM concentration and 15 μM HetR cell concentration for optimal signal:noise sensitivity. All other HetR cell concentrations were 5 μM. The sample cell was loaded with 1.46 mL of degassed HetR and the injection syringe loaded with 0.6 mL of PatS peptide. Blank reference titrations were recorded for each PatS peptide to account for the heats of dilution into sample buffer. Titrations were performed in duplicate and consisted of 35 8 μL injections following an initial 4 μL injection.

RESULTS

EMSA Knockdown Comparison of Native PatS Peptides. HetR has been shown to bind to a 29-base-pair inverted-repeat-containing DNA sequence in the promoter region of *hetP*, a gene encoding a protein that is involved in regulating heterocyst differentiation downstream of HetR.[17,36] This 29-mer DNA substrate containing the inverted repeat (5′-GAGGGGTCTAACCCCTC-3′) was recently used to assess the stoichiometry of HetR-DNA/PatS-5 complexes in EMSA experiments.[17] Here, we used the *hetP*-29-mer to study disruption of HetR binding to DNA by various length C-terminal PatS fragments. In the absence of added PatS, we observed completely shifted DNA by EMSA at 3:1 ratios of HetR:DNA or greater (Figure 1). At or above this ratio, an additional supershifted species was observed for the HetR-*hetP*-29-mer complex. PatS-5 disrupted the supershifted species at a 0.5:1 ratio (PatS:HetR) and completely knocked down the shifted species at a 10:1 ratio.[17] Here, we incubated the 4:1 ratio HetR-*hetP*-29-mer complex separately with 1:1 ratios of PatS-5, PatS-6, PatS-7, and PatS-8 (Figure 1). We observed qualitatively that PatS-7 had a similar disruptive effect on HetR DNA binding activity as PatS-5. Surprisingly, PatS-6 disrupted all shifted DNA at a 1:1 ratio, whereas PatS-8 failed to disrupt HetR/DNA shifts at all. This result was unexpected based on assumptions from an earlier report that a strain of *Anabaena* expressing the PatS-8 minigene on a plasmid was still capable of inhibiting heterocyst differentiation.[37] This result provides indirect evidence that PatS must be processed to a fragment shorter than PatS-8 in order to be active *in vivo*.

Thermodynamics and Binding Affinities of Native and Mutant PatS Peptides Binding to HetR. The observation that disruption of HetR binding to DNA depended on the length of the native PatS C-terminal peptides in EMSA experiments prompted us to quantitatively determine the binding affinities between HetR and each peptide using isothermal titration calorimetry (ITC). We have previously reported ITC data for HetR binding to PatS-5.[17] Here, ITC titration experiments were initially performed with PatS-6, PatS-7, and PatS-8, all using the same batch of HetR. All resulting ITC data were fit with a single binding site model, which allowed determination of the binding stoichiometry n, association constant K_a, and enthalpy of binding $\Delta H°$ (Figure 2 and Table 1). The $\Delta G°$ was determined from K_a, the dissociation constants determined from the inverse of K_a, and $\Delta S°$ calculated using $\Delta G°$ and $\Delta H°$ values. Each PatS peptide bound to HetR in a 1:1 ratio with the exception of PatS-8, for which we could not detect any heats of binding, in agreement with the EMSA observations (PatS-8 also had undetectable binding by ITC and EMSA under reducing conditions of

dx.doi.org/10.1021/bi300228n | *Biochemistry* 2012, 51, 2436−2442

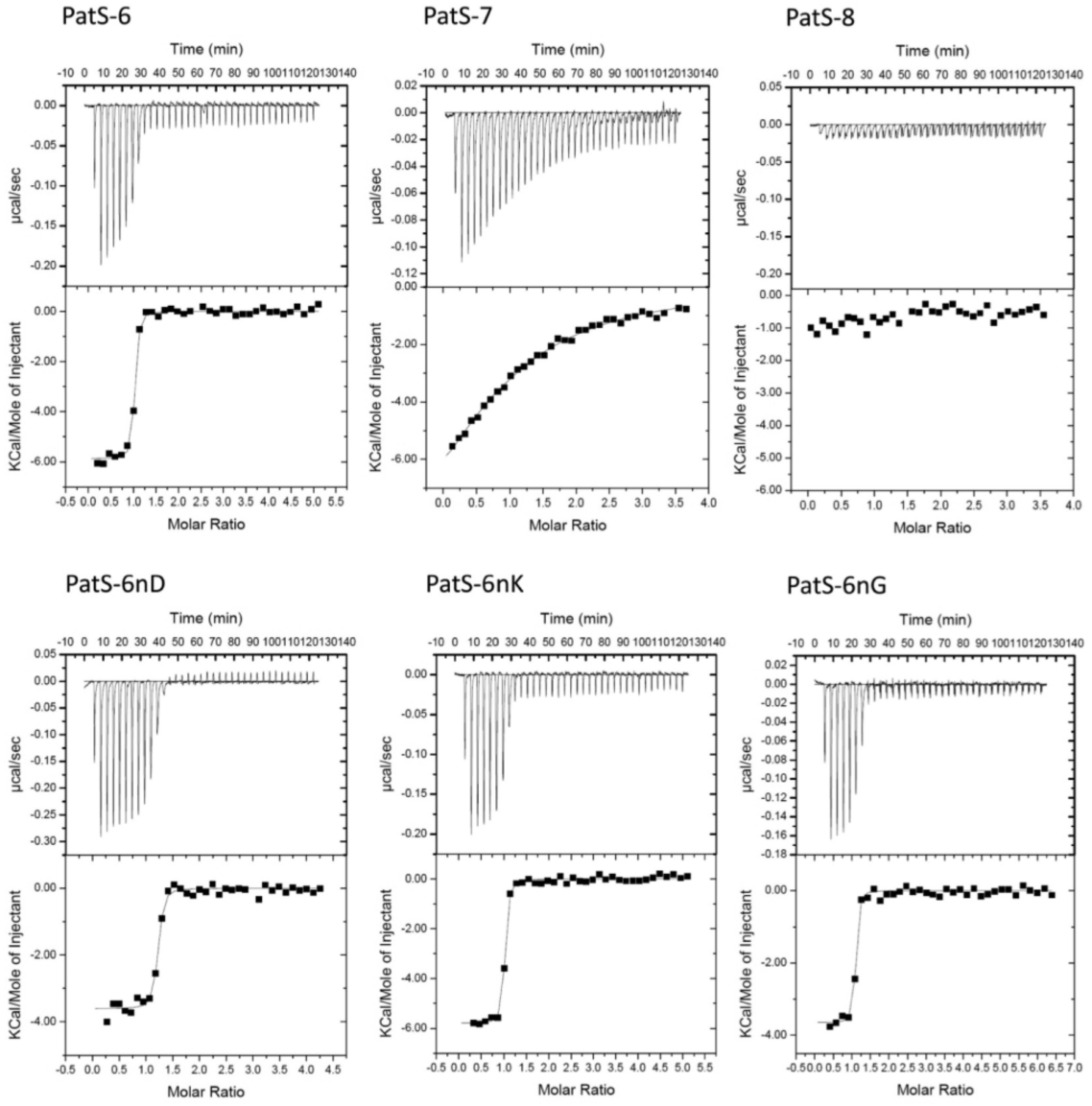

Figure 2. Representative raw and fit ITC isotherms for PatS peptides titrated into HetR. Shown at the top are the raw data for PatS ligands titrated into HetR solutions, and the bottom shows the processed binding isotherms calculated using the best-fit parameters for single binding site models. Experiments were performed in duplicate at 25 °C.

Table 1. Summary of ITC Data for PatS C-Terminal Peptides Titrated into HetR Solutions[a]

peptide	n (no. of sites)	K_d (nM)	$\Delta G°$ (kcal/mol)	$\Delta H°$ (kcal/mol)	$T\Delta S°$ (kcal/mol)
PatS-5*	1.04 ± 0.01*	227 ± 23*	−9.06 ± 0.06*	−8.34 ± 0.41*	0.73 ± 0.46*
PatS-6	0.99 ± 0.02	7.36 ± 0.45	−11.05 ± 0.08	−5.85 ± 0.03	5.25 ± 0.05
PatS-6nD	1.17 ± 0.01	25.7 ± 2.6	−10.36 ± 0.08	−3.60 ± 0.01	6.75 ± 0.07
PatS-6nK	0.97 ± 0.01	5.71 ± 1.33	−11.25 ± 0.14	−5.85 ± 0.04	5.44 ± 0.11
PatS-6nG	1.04 ± 0.01	7.88 ± 1.55	−11.07 ± 0.12	−3.68 ± 0.03	7.39 ± 0.15
PatS-7	0.95 ± 0.02	9280 ± 2430	−6.90 ± 0.16	−12.77 ± 0.23	−5.87 ± 0.39

[a]Errors are reported as the standard deviation between measurements for each set of titrations.The asterisk represents data reported previously.[17]

dithiothreitol, data not shown). The ITC results for PatS-6 indicated surprisingly tight binding between PatS-6 and HetR (K_d = 7.36 ± 0.45 nM), representing a >30-fold increase in affinity compared to PatS-5 (K_d = 227 ± 23 nM).[17] Furthermore, a >1200-fold reduction in binding affinity was observed for PatS-7 (K_d = 9.28 ± 2.43 μM) compared to PatS-6 (and 40-fold reduction compared to PatS-5). The relative HetR binding affinities to PatS-5 and PatS-7 were not discernible from the EMSA data alone since PatS-7 and PatS-5 appeared to similarly disrupt HetR DNA binding activity (Figure 1). The ITC data indicated that HetR binding to PatS-5, PatS-6, and PatS-7 was strongly exothermic for all binding reactions, driven primarily by enthalpic contributions compared with entropic contributions, with the exception of PatS-6 which had comparable magnitudes of binding entropy and binding enthalpy ($\Delta H°$ = −5.85 ± 0.03 kcal/mol and $T\Delta S°$ = 5.25

dx.doi.org/10.1021/bi300228n | *Biochemistry* 2012, 51, 2436−2442

± 0.05 kcal/mol). PatS-6, however, had a larger overall Gibbs free energy (ΔG° = −11.05 ± 0.08 kcal/mol) compared to PatS-5. PatS-7 was the only ligand that exhibited a negative entropic contribution to binding ($T\Delta S^\circ$ = −5.87 ± 0.39 kcal/mol) and a larger magnitude in enthalpy of binding (ΔH° = −12.77 ± 0.23 kcal/mol) compared to the overall Gibbs free energy (ΔG° = −6.90 ± 0.16 kcal/mol).

Having discovered that the N-terminal glutamate residue of PatS-6 conferred more than an order of magnitude tighter binding to HetR compared to PatS-5, we next investigated specifically whether the glutamate residue was necessary for tighter binding or whether other amino acids in this position would maintain high affinity. To address this question, we designed a series of PatS-6 peptides containing various amino acid substitutions at the N-terminal position to determine whether the charge and/or size of the amino acid side chain was essential for increased binding affinity to HetR. The altered peptides included a conservative substitution with another negatively charged amino acid, aspartic acid (PatS-6nD, DRGSGR), substitution of glutamate with a positively charged amino acid, lysine (PatS-6nK, KRGSGR), and substitution with a neutral charged amino acid that lacked a side chain altogether, glycine (PatS-6nG, GRGSGR). ITC titrations of HetR were repeated with these peptides, and the results are shown in Figure 2. Each PatS-6 N-terminal variant bound HetR with a 1:1 stoichiometry and exhibited a highly exergonic Gibbs free energy (Figure 2 and Table 1). PatS-6nK, with its N-terminal substitution of a long-chain positively charged lysine, had a comparable binding affinity (K_d = 5.71 ± 1.33 nM) and thermodynamic parameters (ΔH° = −5.85 ± 0.04 kcal/mol, $T\Delta S^\circ$ = 5.44 ± 0.11 kcal/mol, and ΔG° = −11.25 ± 0.14 kcal/mol) compared to the native PatS-6. Similarly, PatS-6nG also had a comparable binding affinity (K_d = 7.88 ± 1.55 nM) and Gibbs free energy (ΔG° = −11.07 ± 0.12 kcal/mol) despite replacing the negatively charged glutamate with an uncharged glycine that lacked a side chain entirely. However, the enthalpic contribution for PatS-6nG binding was reduced by nearly 40% (ΔH° = −3.68 ± 0.03 kcal/mol), and the entropic contribution was increased by 40% ($T\Delta S^\circ$ = 7.39 ± 0.15 kcal/mol), indicating an entropically rather than an enthalpically driven binding event. To our further surprise, PatS-6nD bind to HetR with a ∼3.5-fold reduced binding affinity (K_d = 25.7 ± 2.6 nM) compared to native PatS-6, despite the conservative substitution with aspartic acid. The Gibbs free energy (ΔG° = −10.36 ± 0.08 kcal/mol) remained consistent with the native PatS-6 and the other PatS-6 variants, yet similarly to the shorter PatS-6nG, the enthalpic contribution was reduced by nearly 40% (ΔH° = −3.60 ± 0.01 kcal/mol) and the entropic contribution was increased by 30% ($T\Delta S^\circ$ = 6.75 ± 0.07 kcal/mol), resulting in an entropically driven interaction.

EPR Spectroscopy of Spin-Labeled HetR Titrated with PatS-6. Continuous wave (CW) EPR was used to study PatS-6 binding to a HetR double mutant (C48A, L252C) spin-labeled with the nitroxide free radical probe MTSL on the cysteine at residue 252. We have previously shown that the CW EPR spectrum of this spin-label HetR mutant experiences motional averaging that is quenched when HetR binds to PatS-5.[17] Here, similarly as with PatS-5, we observed significant quenching of the conformational dynamics of the electron radical associated with the MTSL nitroxide group attached to 252C (Figure 3). However, binding to PatS-6 quenched the spin-label motion at a 10-fold lower concentration compared to PatS-5 (i.e., at a 1:1 ratio compared with a 10:1 ratio in the previous PatS-5 study[17]). The local rotational diffusion rate of the MTSL electron radical in the PatS-6 bound state approached R_{iso} = 9.12 × 10^5 s^{-1} compared to the free state (R_{iso} = 5.25 × 10^6 s^{-1}) (simulation parameters are in Table 2), indicating almost an order of magnitude reduction in the local rotational diffusion rate of the spin-label after binding to PatS-6. PatS-8 was titrated to a 10:1 excess into a spin-labeled sample of HetR 252C; however, no quenching of motion was observed (data not shown), serving as another negative control similar to the Poly-G pentapeptide (GGGGG) used previously.[17] Taken together, the site-directed spin-labeling CW EPR titration data were in strong agreement with the observed EMSA and ITC data, indicating that HetR has a much higher affinity for PatS-6 compared to PatS-5.

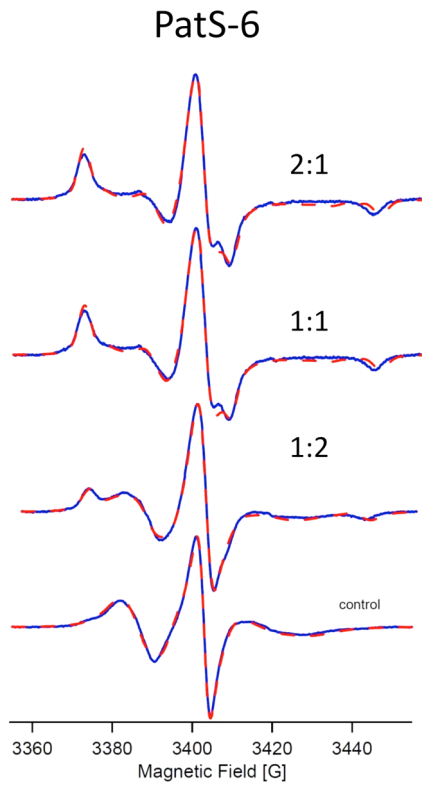

Figure 3. CW EPR spectra of PatS-6 titrations into the HetR 252C mutant spin-labeled with MTSL. The control spectrum of HetR at 200 μM concentration is shown at the bottom. The remaining spectra consist of PatS-6 titrated into the HetR solution at increasing stoichiometric ratios (indicated above each spectrum). CW X-band EPR spectra were recorded at room temperature. Experimental data are represented by the solid blue lines, and best-fit data simulations are represented by the red dashed lines.

DISCUSSION

While the functional forms of PatS and HetN that regulate formation of patterns of heterocysts in filamentous cyanobacteria remain unknown, PatS-5 has served as a surrogate for the full-length PatS peptide since its discovery as the minimally required PatS peptide fragment for normal patterns of heterocyst differentiation, and recent evidence suggests that the PatS-5 sequence found in HetN is also required for HetN function.[11,38] However, here we have shown that PatS-6 binds HetR with a 30-fold greater affinity compared to PatS-5, suggesting that the interaction of HetR with PatS-6 may be the more efficient of the two, and raising the alternative possibility

Table 2. Simulation Parameters for CW EPR Data of the PatS-6 Titration into a Solution of HetR 252C Mutant Spin-Labeled with MTSL

sample		A_{xx} (G)	A_{yy} (G)	A_{zz} (G)	g_{xx}	g_{yy}	g_{zz}	log(R_{xx})	log(R_{yy})	log(R_{zz})	log(R_{iso})	β (deg)	% site 1	% site 2
control		7.24	5.94	35.55	2.0083	2.0049	2.0023	7.49	8.43	4.25	6.72	27.67	100.00	0.00
+PatS-6 1:2	site 1	7.24	5.94	35.55	2.0083	2.0049	2.0023	6.83	8.53	4.20	6.52	22.48	52.11	47.89
	site 2	7.24	5.94	35.55	2.0083	2.0049	2.0023	4.63	6.17	7.64	6.15	2.27		
+PatS-6 1:1	site 1	7.24	5.94	35.55	2.0083	2.0049	2.0023	6.88	8.54	4.25	6.56	22.49	18.62	81.38
	site 2	7.24	5.94	35.55	2.0083	2.0049	2.0023	4.59	6.06	7.59	6.08	2.28		
+PatS-6 2:1	site 1	7.24	5.94	35.55	2.0083	2.0049	2.0023	6.88	8.54	4.25	6.56	22.49	15.12	84.88
	site 2	7.24	5.94	35.55	2.0083	2.0049	2.0023	4.22	6.07	7.60	5.96	2.28		

that PatS-6 might be the active processed form of PatS *in vivo* instead of PatS-5. Our results clearly indicated that the length of the PatS sequence, in this case PatS-5 (RGSGR), PatS-6 (ERGSGR), PatS-7 (DERGSGR), or PatS-8 (CDERGSGR), has the potential to play a critical role in regulating heterocyst differentiation inhibition based on observed differences in their binding affinities to HetR. Since the active forms of PatS or HetN have not, to date, been successfully isolated, it is plausible that any one of these inhibitory sequences may accumulate as a result of protease processing machinery and regulate heterocyst differentiation via the aforementioned gradient of inhibitors that promote destruction of HetR and other positive regulatory factors. However, processing at least to PatS-7 sequences or shorter appear to be minimally required to enable a binding interaction between HetR and PatS fragments. The biological significance of these findings remains to be shown, and testing these hypotheses will require further *in vivo* studies.

After the discovery that HetR has significantly higher affinity for PatS-6 compared to PatS-5, we set out to understand the biophysical factors that contribute to the tighter binding. One obvious question that needed to be answered was whether or not the naturally occurring N-terminal glutamate in PatS-6 was special or required for the increased binding affinity. We had already been able to elucidate important information about the PatS-HetR binding interaction from the ITC studies for HetR binding to the native PatS peptide sequences. It was clear from the thermodynamics information derived from the ITC data that all HetR-PatS peptide binding interactions were highly exothermic based on calculated ΔH° values. The relatively large negative enthalpy and positive entropy associated with HetR-PatS peptide binding interactions was consistent with ionic interactions and/or formations of hydrogen bonds[30,39−42] in the complexes, which would be expected based on the charged nature of the PatS ligands tested at pH 7.8. In order to explicitly probe the importance of the N-terminal glutamate in PatS-6, three modified PatS-6 sequences were prepared with strategically selected substitutions of the N-terminal glutamate and the binding affinities measured by ITC and compared to the native PatS-6 peptide. Surprisingly, replacing the native N-terminal glutamate of PatS-6 with a long chain positively charged lysine did not compromise the tight binding affinity of HetR, indicating that the negatively charged glutamate carboxyl side chain did not make an important contribution to the tight binding observed between PatS-6 and HetR. Since the charge on the N-terminal amino acid side chain did not contribute to increased binding affinity, this left the possibility that the increased affinity was due either to a new hydrophobic interaction with the side chain of the N-terminal residue of PatS-6 or due to a new polar interaction, likely a hydrogen bond, between HetR and the additional peptide backbone formed between the N-terminal residue and the first arginine residue in the RSGSR segment. These possibilities were clearly addressed using data collected for a PatS-6 sequence that contained a substitution of the N-terminal glutamate with a neutral charged amino acid that lacked a side chain altogether, namely the glycine residue in PatS-6nG. The ITC data for the PatS-6nG indicated that HetR bound to this peptide without any loss in binding affinity compared to the native PatS-6 sequence. This result indicated that the length and/or nature of the side chain was not important for binding to HetR, ruling out the importance of a new hydrophobic interaction. Rather, the data indicated that the N-terminal residue confers increased binding affinity with HetR purely through a new peptide backbone interaction, possibly through the formation of new hydrogen bonds. While the ITC data on the various length native PatS peptide fragments and on the PatS-6 peptides that contained various N-terminal amino acid substitutions have shed important light regarding the specific interactions between HetR and PatS, the detailed molecular level understanding of the relative binding affinities of the PatS peptides will only be fully realized once the three-dimensional structures of the complexes become available.

AUTHOR INFORMATION

Corresponding Author

*Tel: (513)-529-8267; Fax: (513)-529-5715; e-mail kennedm4@muohio.edu.

Funding

This work was supported in part by a grant from NSF (IOS-0919878) to S.M.C.

Notes

The authors declare no competing financial interest.

ACKNOWLEDGMENTS

The authors thank Professor Susan Barnum for providing the genomic DNA of *Anabaena* sp. strain PCC 7120 and Kelly Higa and Patrick Videau for insightful discussions.

REFERENCES

(1) Brocks, J. J., Logan, G. A., Buick, R., and Summons, R. E. (1999) Archean molecular fossils and the early rise of eukaryotes. *Science 285*, 1033−1036.

(2) Wolk, C. P. (1996) Heterocyst formation. *Annu. Rev. Genet. 30*, 59−78.

(3) Meeks, J. C., Wolk, C. P., Lockau, W., Schilling, N., Shaffer, P. W., and Chien, W. S. (1978) Pathways of assimilation of [13N]N2 and 13NH4+ by cyanobacteria with and without heterocysts. *J. Bacteriol. 134*, 125−130.

(4) Burris, R. H., and Roberts, G. P. (1993) Biological nitrogen fixation. *Annu. Rev. Nutr. 13*, 317−335.

(5) Wolk, C. P., Ernst, A., and Elhai, J. (1994) *Heterocyst Metabolism and Development*, Vol. *1*, Kluwer Academic Publishers, Dordrecht, The Netherlands.

(6) Wolk, C. P., and Quine, M. P. (1975) Formation of one-dimensional patterns by stochastic processes and by filamentous blue-green algae. *Dev. Biol. 46*, 370−382.
(7) Flores, E., and Herrero, A. (2010) Compartmentalized function through cell differentiation in filamentous cyanobacteria. *Nat. Rev. Microbiol. 8*, 39−50.
(8) Golden, J. W., and Yoon, H. S. (2003) Heterocyst development in Anabaena. *Curr. Opin. Microbiol. 6*, 557−563.
(9) Wilcox, M., Mitchison, G. J., and Smith, R. J. (1973) Pattern formation in the blue-green alga, Anabaena. I. Basic mechanisms. *J. Cell Sci. 12*, 707−723.
(10) Wilcox, M., Mitchison, G. J., and Smith, R. J. (1973) Pattern formation in the blue-green alga Anabaena. II. Controlled proheterocyst regression. *J. Cell Sci. 13*, 637−649.
(11) Risser, D. D., and Callahan, S. M. (2009) Genetic and cytological evidence that heterocyst patterning is regulated by inhibitor gradients that promote activator decay. *Proc. Natl. Acad. Sci. U. S. A. 106*, 19884−19888.
(12) Yoon, H. S., and Golden, J. W. (1998) Heterocyst pattern formation controlled by a diffusible peptide. *Science 282*, 935−938.
(13) Yoon, H. S., and Golden, J. W. (2001) PatS and products of nitrogen fixation control heterocyst pattern. *J. Bacteriol. 183*, 2605−2613.
(14) Callahan, S. M., and Buikema, W. J. (2001) The role of HetN in maintenance of the heterocyst pattern in Anabaena sp. PCC 7120. *Mol. Microbiol. 40*, 941−950.
(15) Buikema, W. J., and Haselkorn, R. (1991) Characterization of a gene controlling heterocyst differentiation in the cyanobacterium Anabaena 7120. *Genes Dev. 5*, 321−330.
(16) Rajagopalan, R., and Callahan, S. M. (2010) Temporal and spatial regulation of the four transcription start sites of hetR from Anabaena sp. strain PCC 7120. *J. Bacteriol. 192*, 1088−1096.
(17) Feldmann, E. A., Ni, S., Sahu, I. D., Mishler, C. H., Risser, D. D., Murakami, J. L., Tom, S. K., McCarrick, R. M., Lorigan, G. A., Tolbert, B. S., Callahan, S. M., and Kennedy, M. A. (2011) Evidence for Direct Binding between HetR from Anabaena sp. PCC 7120 and PatS-5. *Biochemistry 50*, 9212−9224.
(18) Black, T. A., Cai, Y., and Wolk, C. P. (1993) Spatial expression and autoregulation of hetR, a gene involved in the control of heterocyst development in Anabaena. *Mol. Microbiol. 9*, 77−84.
(19) Zhou, R., Cao, Z., and Zhao, J. (1998) Characterization of HetR protein turnover in Anabaena sp. PCC 7120. *Arch. Microbiol. 169*, 417−423.
(20) Buikema, W. J., and Haselkorn, R. (2001) Expression of the Anabaena hetR gene from a copper-regulated promoter leads to heterocyst differentiation under repressing conditions. *Proc. Natl. Acad. Sci. U. S. A. 98*, 2729−2734.
(21) Muro-Pastor, A. M., Valladares, A., Flores, E., and Herrero, A. (2002) Mutual dependence of the expression of the cell differentiation regulatory protein HetR and the global nitrogen regulator NtcA during heterocyst development. *Mol. Microbiol. 44*, 1377−1385.
(22) Ehira, S., and Ohmori, M. (2006) NrrA directly regulates expression of hetR during heterocyst differentiation in the cyanobacterium Anabaena sp. strain PCC 7120. *J. Bacteriol. 188*, 8520−8525.
(23) Ehira, S., and Ohmori, M. (2006) NrrA, a nitrogen-responsive response regulator facilitates heterocyst development in the cyanobacterium Anabaena sp. strain PCC 7120. *Mol. Microbiol. 59*, 1692−1703.
(24) Laurent, S., Chen, H., Bédu, S., Ziarelli, F., Peng, L., and Zhang, C. C. (2005) Nonmetabolizable analogue of 2-oxoglutarate elicits heterocyst differentiation under repressive conditions in Anabaena sp. PCC 7120. *Proc. Natl. Acad. Sci. U. S. A. 102*, 9907−9912.
(25) Huang, X., Dong, Y., and Zhao, J. (2004) HetR homodimer is a DNA-binding protein required for heterocyst differentiation, and the DNA-binding activity is inhibited by PatS. *Proc. Natl. Acad. Sci. U. S. A. 101*, 4848−4853.
(26) Risser, D. D., and Callahan, S. M. (2007) Mutagenesis of hetR reveals amino acids necessary for HetR function in the heterocystous cyanobacterium Anabaena sp. strain PCC 7120. *J. Bacteriol. 189*, 2460−2467.
(27) Kim, Y., Joachimiak, G., Ye, Z., Binkowski, T. A., Zhang, R., Gornicki, P., Callahan, S. M., Hess, W. R., Haselkorn, R., and Joachimiak, A. (2011) Structure of transcription factor HetR required for heterocyst differentiation in cyanobacteria. *Proc. Natl. Acad. Sci. U. S. A. 108*, 10109−10114.
(28) Falconer, R. J., Penkova, A., Jelesarov, I., and Collins, B. M. (2010) Survey of the year 2008: applications of isothermal titration calorimetry. *J. Mol. Recognit. 23*, 395−413.
(29) Choi, H. J., Gross, J. C., Pokutta, S., and Weis, W. I. (2009) Interactions of plakoglobin and beta-catenin with desmosomal cadherins: basis of selective exclusion of alpha- and beta-catenin from desmosomes. *J. Biol. Chem. 284*, 31776−31788.
(30) Grässlin, A., Amoreira, C., Baldridge, K. K., and Robinson, J. A. (2009) Thermodynamic and computational studies on the binding of p53-derived peptides and peptidomimetic inhibitors to HDM2. *ChemBioChem 10*, 1360−1368.
(31) Schneider, D., and Freed, J. (1989) Calculating slow motional magnetic resonance spectra: A user's guide, in *Biological Magnetic Resonance* (Berliner, L., and Reuben, J., Eds.) pp 1−76, Plenum, New York.
(32) Budil, D., Lee, S., Saxena, S., and Freed, J. (1996) Nonlinear-least-squares analysis of slow-motion EPR spectra in one and two dimensions using a modified Levenberg-Marquardt algorithm. *J. Magn. Reson., Ser. A*, 155−189.
(33) Hoofnagle, A. N., Stoner, J. W., Lee, T., Eaton, S. S., and Ahn, N. G. (2004) Phosphorylation-dependent changes in structure and dynamics in ERK2 detected by SDSL and EPR. *Biophys. J. 86*, 395−403.
(34) Zhang, Z., Fleissner, M. R., Tipikin, D. S., Liang, Z., Moscicki, J. K., Earle, K. A., Hubbell, W. L., and Freed, J. H. (2010) Multifrequency electron spin resonance study of the dynamics of spin labeled T4 lysozyme. *J. Phys. Chem. B 114*, 5503−5521.
(35) Nesmelov, Y. E., Agafonov, R. V., Burr, A. R., Weber, R. T., and Thomas, D. D. (2008) Structure and dynamics of the force-generating domain of myosin probed by multifrequency electron paramagnetic resonance. *Biophys. J. 95*, 247−256.
(36) Higa, K. C., and Callahan, S. M. (2010) Ectopic expression of hetP can partially bypass the need for hetR in heterocyst differentiation by Anabaena sp. strain PCC 7120. *Mol. Microbiol. 77*, 562−574.
(37) Wu, X., Liu, D., Lee, M. H., and Golden, J. W. (2004) patS minigenes inhibit heterocyst development of Anabaena sp. strain PCC 7120. *J. Bacteriol. 186*, 6422−6429.
(38) Higa, K. C., Rajagopalan, R., Risser, D. D., Rivers, O. S., Tom, S. K., Videau, P., and Callahan, S. M. (2012) The RGSGR amino acid motif of the intercellular signalling protein, HetN, is required for patterning of heterocysts in Anabaena sp. strain PCC 7120. *Mol. Microbiol. 83*, 682−693.
(39) Ross, P. D., and Subramanian, S. (1981) Thermodynamics of protein association reactions: forces contributing to stability. *Biochemistry 20*, 3096−3102.
(40) Connelly, P. R., Aldape, R. A., Bruzzese, F. J., Chambers, S. P., Fitzgibbon, M. J., Fleming, M. A., Itoh, S., Livingston, D. J., Navia, M. A., and Thomson, J. A. (1994) Enthalpy of hydrogen bond formation in a protein-ligand binding reaction. *Proc. Natl. Acad. Sci. U. S. A. 91*, 1964−1968.
(41) Calderone, C. T., and Williams, D. H. (2001) An enthalpic component in cooperativity: the relationship between enthalpy, entropy, and noncovalent structure in weak associations. *J. Am. Chem. Soc. 123*, 6262−6267.
(42) Williams, D. H., Stephens, E., O'Brien, D. P., and Zhou, M. (2004) Understanding noncovalent interactions: ligand binding energy and catalytic efficiency from ligand-induced reductions in motion within receptors and enzymes. *Angew. Chem., Int. Ed. 43*, 6596−6616.